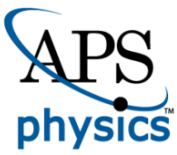

Importance Sampling of Randomized Measurements for Probing Entanglement

Aniket Rath, Rick van Bijnen, Andreas Elben, Peter Zoller, and Benoît Vermersch

Phys. Rev. Lett. **127**, 200503 — Published 11 November 2021

DOI: 10.1103/PhysRevLett.127.200503

Importance sampling of randomized measurements for probing entanglement

Aniket Rath,[1] Rick van Bijnen,[2,3] Andreas Elben,[2,3] Peter Zoller,[2,3] and Benoît Vermersch[1,2,3]

[1] *Univ. Grenoble Alpes, CNRS, LPMMC, 38000 Grenoble, France*

[2] *Center for Quantum Physics, University of Innsbruck, Innsbruck A-6020, Austria*

[3] *Institute for Quantum Optics and Quantum Information of the Austrian Academy of Sciences, Innsbruck A-6020, Austria*

We show that combining randomized measurement protocols with importance sampling allows for characterizing entanglement in significantly larger quantum systems and in a more efficient way than in previous work. A drastic reduction of statistical errors is obtained using classical techniques of machine-learning and tensor networks using partial information on the quantum state. In current experimental settings of engineered many-body quantum systems this significantly increases the (sub-)system sizes for which entanglement can be measured. In particular, we show an exponential reduction of the required number of measurements to estimate the purity of product states and GHZ states.

Measuring the properties of many-body states, and in particular quantifying entanglement for increasing system sizes is a key challenge in assessing and utilizing the power of large-scale quantum computers [1] and simulators [2, 3]. The recent development of *randomized measurements* provides us with a general toolbox to measure in a state-agnostic way physical quantities associated with entanglement [4–17], scrambling [18–20], topological order [21, 22], and in cross-device quantum verification [23]. Randomized measurements are particularly well suited to current experimental settings, requiring only (random) single qubit rotations and site-resolved measurements. Moreover, estimations are made directly from the measured data, with low number of measurements compared to tomography [24]. These protocols have enabled in recent experimental work the measurement of (entanglement) Rényi entropies [16, 25], negativities [12], state-fidelities [23], and scrambling [26].

While these experiments have been performed in the regime of subsystems with ten particles, the ongoing development of quantum systems involving hundreds of qubits [1–3] raises the challenge to scale these protocols to significantly larger (sub-)system sizes. The current bottleneck is the required number of measurements to overcome statistical errors: For instance, the number of randomized measurements to estimate the purity with a given accuracy is of the order of 2^{aN} for a (sub-)system of N qubits, with $a \approx 1$ [6, 11]. In this letter, we show that importance sampling will allow us to push randomized protocols to study significantly larger (sub-)system sizes. In particular, our scaling analysis for product states and GHZ states shows that the required number of measurements $2^{a'N}$ has a reduced exponent $a' < a$ compared to our previous 'uniform' sampling approach. We also observe below significant reductions of statistical errors when estimating with importance sampling the purity of random states, and highly entangled states created by a quantum quench.

While our approach can be realized in any randomized measurement protocol, we consider for concreteness the situation of probing entanglement for a bipartite quantum system A and B. Our aim is to measure the purities $p_2 = \mathrm{Tr}(\rho^2)$, and second Rényi entropies $S_2 = -\log(p_2)$ of a subsystem A of N qubits described by a reduced density matrix ρ. The values of p_2 and S_2 can be used to quantify entanglement [27], but also to unravel universal aspects of many-body quantum matter [28]. Using the protocol presented in this Letter, the number of measurements to access the purity in existing setups can be exponentially reduced, allowing for instance to probe topological order on large-scale surface codes [29], or to verify in a state-agnostic way large quantum circuits [23, 30].

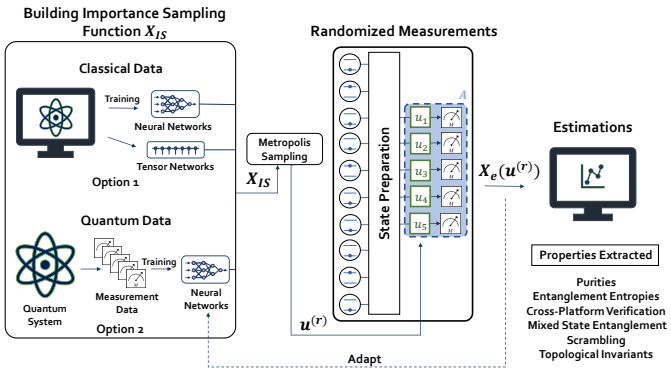

FIG. 1. *Randomized measurement protocol with importance sampling.* In the first phase, we construct a classical function $X_{\mathrm{IS}}(u)$. In the second phase, unitaries are sampled from the appropriate classical representation. In the last phase, measurements are performed in the quantum system, and are analyzed to construct different properties accessible by randomized measurements. The measurement data obtained during the experiment could also be considered as additional samples to obtain improved classical function for future experiments.

The purity p_2 can be written as an integral $p_2 = \int X(u)du$ of the quantity [6, 8, 25]

$$X(u) = 2^N \sum_{s,s'} (-2)^{-D[s,s']} P_u(s) P_u(s'), \qquad (1)$$

with the integration performed over all local unitary transformations $u = u_1 \otimes \cdots \otimes u_N$, with respect to

the Haar measure $du = \Pi_i du_i$ (see Supplemental Material (SM) [31]). Here, $P_u(s) = \langle s| u\rho u^\dagger |s\rangle$ are the probabilities of measuring a particular bitstring s in the computational basis after rotation u (c.f. Fig 1), and D is the Hamming distance. In practice, the purity can be evaluated using a Monte Carlo integration $p_2 \approx (N_u)^{-1} \sum_r X(u^{(r)})$, obtained by uniformly sampling a finite number of local transformations $u^{(r)} = u_1^{(r)} \otimes \cdots \otimes u_N^{(r)}$ $(r = 1, \ldots, N_u)$.

Statistical errors in the estimation of the purity are due to both shot noise (the finite number of measurement samples N_M used to estimate the probabilities $P_u(s)$), and to the finite number of transformations N_u. The challenge to overcome statistical errors is related to the fact that the function $X(u)$ takes values in an exponentially large interval $[2^{-N}, 2^N]$ (see SM [31]). Here, we propose to sample unitaries from a distribution $p_{\rm IS}$ that prioritizes the 'important' regions of X giving larger contributions to the total integral (1), and we write the purity as

$$p_2 = \int \left(\frac{X(u)}{p_{\rm IS}(u)} \right) p_{\rm IS}(u) du. \tag{2}$$

The gain in estimating the purity via Monte Carlo integration with importance sampling becomes apparent when quantifying the statistical error $\mathcal{E}$ in measuring p_2 for $N_M \to \infty$ with a finite number of unitaries N_u, being of the order of $\mathrm{std}_{\rm IS}(X/p_{\rm IS})/\sqrt{N_u}$, when compared with uniform sampling $\mathrm{std}(X)/\sqrt{N_u}$ [33]. Here std and $\mathrm{std}_{\rm IS}$ are the standard deviations according to the Haar measure du, and the distribution $p_{\rm IS}(u)du$, respectively.

Our protocol is summarized in Fig. 1. (i) *Building* $X_{\rm IS}$: We first construct on a classical computer an approximation $X_{\rm IS}(u)$ of the function $X(u)$. This function can be built based on partial information on the quantum state (classical data). We can also form $X_{\rm IS}(u)$ from measurements performed on a quantum system (quantum data). This can be data from prior experiments under study, but could also be data from another experiment, potentially a more noisy quantum device or platform running the same quantum task. (ii) *Sampling*: We define a probability distribution $p_{\rm IS}(u) = |X_{\rm IS}(u)|/\int |X_{\rm IS}(u)| du$ [34], and sample a set of N_u random unitaries via the Metropolis algorithm [33]. (iii) *Measurements*: For each $u^{(r)}$, we collect $m = 1, \ldots, N_M$ bitstrings $s_m^{(r)}$ from randomized measurements performed on the quantum device. (iv) *Estimation*: As the bistrings $s_m^{(r)}$ are distributed according to the probabilities $P_{u^{(r)}}(s)$, we use Eq. (1), and construct an unbiased estimation of $X(u^{(r)})$

$$X_e(u^{(r)}) = \frac{2^N}{N_M(N_M-1)} \sum_{m \neq m'} (-2)^{-D[s_m^{(r)}, s_{m'}^{(r)}]}, \tag{3}$$

which only differs from $X(u^{(r)})$ due to shot noise. Averaging $(X_e(u^{(r)})/p_{\rm IS}(u^{(r)}))$ over the unitaries $u^{(r)}$, $r = 1, \ldots, N_u$, we obtain an estimation of the purity $[p_2]_{\rm IS}$.

Importance sampling reduces the total required number of measurements $N_u N_M$ associated with a given statistical error $\mathcal{E}$. When sampling unitaries u according to $p_{\rm IS}$, we first reduce the required number of unitaries N_u to achieve $\mathcal{E}$ in the limit $N_M \to \infty$, as discussed above. In addition, the number of shots N_M required to satisfy an error threshold is also less compared to uniform sampling. The intuition behind this result is that the unitaries u sampled according to $p_{\rm IS}$ are preferentially chosen in the vicinity of the maximum of X, where the effect of shot noise is minimal. For instance, with a product state, the maximum value of $X(u)$ is obtained when the distribution is peaked as $P_u(s) = \delta_{s,s_0}$ (see SM [31]), i.e., when one shot only $N_M = 1$ is sufficient to obtain convergence $X_e(u) = X(u)$. When estimating the purity by averaging $X_e(u)$ over $p_{\rm IS}$, we indeed numerically observe, for product and GHZ states, an exponential reduction of the required value of N_M.

Task (i) of our protocol is the crucial part governing the efficiency of our protocol. If the quantum state can be represented classically up to unknown decoherence effects, such as for the product state, or a GHZ state, we can build a quasi-exact representation $X_{\rm IS}(u)$ of $X(u)$. Our protocol is also relevant when only approximations $X_{\rm IS}(u)$ of $X(u)$ are available, for instance if we have only access to a mean-field or a variational wavefunction. In particular, we show below that tensor networks [35], which, with limited bond dimension, cannot faithfully represent a highly entangled state, are indeed useful to access the purity with reduced number of measurements compared to uniform sampling. Similarly, when building $X_{\rm IS}(u)$ from quantum data, we can use recent tomographic techniques [24, 36–39], even in situations when they do not accurately represent the quantum state.

The rest of this letter presents a detailed recipe to build the approximation $X_{\rm IS}(u)$ from limited information on the state, as well as performance tests and scaling analyses of statistical errors with various quantum states.

Building the sampler $X_{\rm IS}$—To construct $X_{\rm IS}$, we assume we have access to a finite number $N_{\rm samples}$ of random measurements $X_a(u^{(k)})$, $k = 1, \ldots, N_{\rm samples}$. These measurements can be obtained from *classical data*, i.e., from a representation of the state on a classical computer. $X_a(u^{(k)})$ is only an approximation of the true measurement $X(u^{(k)})$. This can be due to unknown decoherence effects, but also to fundamental reasons that limit our ability to represent classically a quantum state. For instance, we can consider that X_a is generated by a mean-field, variational tensor-network methods [35] (e.g., matrix-product-states (MPS) - two-dimensional projected-entangled pair states (PEPS)) with limited bond dimension, or machine-learning representations [40]. Alternatively, we can also have prior access to the experimental system realizing the quantum

state and measure $X_a(u^{(k)}) = X_e(u^{(k)})$ via Eq. (3) based on *quantum data*, c.f. Fig. 1. Note that step (i) leads to a result that can be saved classically, i.e. this step does not need to be repeated every time we want to probe a given quantum system.

As detailed in SM [31], we can parametrize single qubit random unitaries $u_i = R_y(\theta_i)R_z(\varphi_i)$ in terms of two rotations. The function $X(u)$ we would like to approximate is thus a multivariate function of $2N$ variables θ_i, φ_i, $i = 1, \ldots, N$. In order to construct $X_{\rm IS}(u)$ as an object that can be used for sampling, we rely on machine-learning (ML) techniques of nonlinear multivariate regression. We use existing highly optimized algorithms to fit our samples by a neural network representing our target multivariate function $X_{\rm IS}(u)$. For each sample k, the $2N$ angles $\theta_i^{(k)}, \varphi_i^{(k)}$ parametrizing $u^{(k)}$ are used as inputs of the neural network, while the value of the measured function $X_a(u^{(k)})$ is the output of the network. This provides a 'training' procedure, which results in a fitted neural network $X_{\rm IS}(u)$, which we can finally save and use for the next step of sampling unitaries (ii) of the protocol. Note that, when a theory representation X_a is available, one could define $X_{\rm IS} = X_a$, i.e., avoid fitting with ML and sample directly from X_a. While this approach is probably the most obvious for small systems, using ML offers in the large scale scenario the possibility of converting the result of a very costly classical computation into a neural network $X_{\rm IS}(u)$. This neural network can be seen as a 'compressed object' and can be saved and shared classically on-demand (multiple times and/or for multiple users) to realize the sampling task (ii).

Performance tests— We now benchmark our protocol. For all states that we analyzed, product states, GHZ states, random states and other highly entangled states, we observe a drastic reduction of statistical errors with importance sampling.

We begin by considering product states $\rho = |\psi\rangle\langle\psi|$, with $|\psi\rangle = |0\rangle^{\otimes N}$. We consider having access to classical data with samples of randomized measurements that are not affected by shot-noise. The details of the training procedure are presented in the SM [31]. For such product state, the training of a neural network $X_{\rm IS}(u)$ is straightforward, and we achieve a fit of $X(u)$ using three layers of neurons, with mean absolute error below five percents, see SM [31]. To assess the performance of importance sampling, we will compare the average statistical error $\mathcal{E}$ in estimating the purity, with the one obtained with uniform sampling ($X_{\rm IS} = 1$). We compute $\mathcal{E} = \overline{|p_2 - p_{2e}|}$ by numerically simulating our protocol, with $\bar{}$ an average over simulated experiments. The results are shown in Fig. 2(a). With uniform and importance sampling, the error decays as $1/\sqrt{N_u}$, with a prefactor that is approximately 5 times smaller for importance sampling. We consider GHZ states $|\psi\rangle = (|0\rangle^{\otimes N} + |1\rangle^{\otimes N})/\sqrt{2}$ in Fig. 2(b). Here, importance sampling provides a significant advantage over uniform sampling, meaning that the neural network succeeded in learning how to sample correlated random unitaries that are adapted to probe a GHZ state.

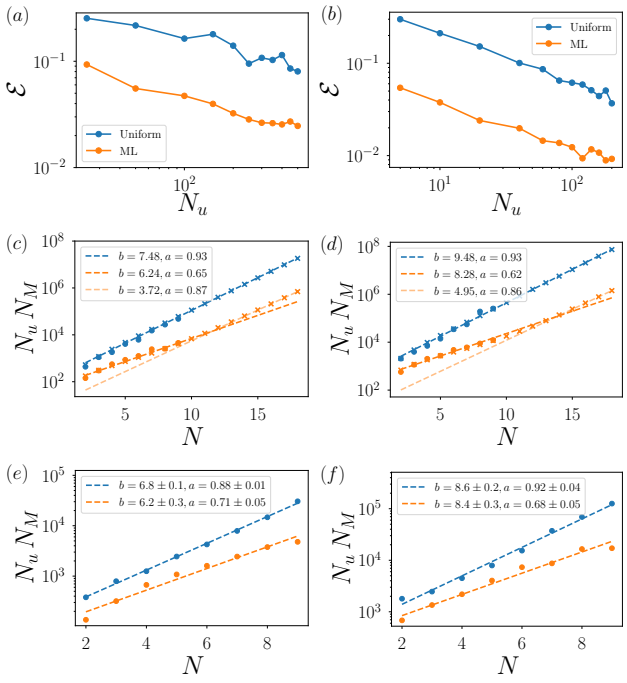

FIG. 2. *Statistical error scalings for product and GHZ states* Average statistical error $\mathcal{E}$ of the estimated purity for (a) 10-qubit product state and (b) 5-qubit GHZ state in function of N_u with $N_M = 1000$ for a uniform sampling (Uniform) and importance sampling from a machine learning model (ML). (c-d) Scaling of the required total number of measurements $N_u N_M$ as a function of N for uniform and importance sampling for a product state, to obtain a statistical error of $\mathcal{E} = 0.1$ (c), and $\mathcal{E} = 0.05$ (d), respectively. We represent with cross the analytical prediction (c.f. SM) and with circles the numerical simulations. Panels (e-f) show the numerical simulations for the GHZ states for $\mathcal{E} = 0.1$ and $\mathcal{E} = 0.05$ with corresponding exponential fits of the type 2^{b+aN}.

We can also extract from numerical simulations the total number of measurements $N_u N_M$, minimized over possible choices of N_u, N_M, that is required to achieve a statistical error $\mathcal{E}$. Here, to ensure that we extract scaling relations that are independent of the choice of the neural network ansatz, with importance sampling, we sample directly from the ideal theory state $X_{\rm IS}(u) = X(u)$. In this case, for a fixed number of measurements, the statistical error is minimized for $N_u = 1$. We present in the SM [31] additional numerical simulations, using optimized neural networks for $N_u = 200, 500$ which support the same conclusions. For the product state, we observe in Fig. 2(c-d) that the required $N_u N_M$ grows as 2^{b+aN} (see also Ref. [25]) with $a \approx 0.93$ for uniform sampling, and $a \approx 0.65$ for importance sampling. Our numerical results for the GHZ states [panels (e)-(f)] show similar results, with favorable scaling exponents for importance

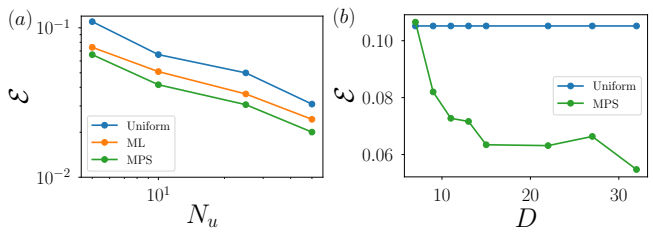

FIG. 3. *Purity estimation of a highly entangled 10 qubit state with ML and MPS samplers.* Panel (a) shows the average statistical error $\mathcal{E}$ of the estimated purity in function of N_u with $N_M = 7500$ for a uniform sampling and importance sampling done from a neural network and a MPS representation of the corresponding state respectively. Panel (b) illustrates the scaling of the error $\mathcal{E}$ w.r.t different bond dimensions D used for the MPS representation of the state for $N_u = 5$ and $N_M = 7500$.

samplings, in particular at high accuracy $\mathcal{E} = 0.05$ [panel (f)]. As the exponent a is reduced compared to uniform sampling, we see that importance sampling offers an exponential reduction of the required number of measurements. In addition, in all panels (c-f), the prefactor 2^b obtained for importance sampling is smaller than the one for uniform sampling.

For pure product states, we can compare our numerical results with analytical calculations, which are presented in the SM [31], and extend them to the large N limit. Our analytical study shows the existence of two regimes: For $N \lesssim N_c$, smaller than a certain value $N_c \propto \log(1/\mathcal{E})$, we find a strongly favorable scaling exponent of $a = 0.37$ for importance sampling. For large $N \gtrsim N_c$, the exponent increases towards $a \approx 0.88$ which is however still smaller than in the case of uniform sampling, $a \approx 0.92$. In particular, we note that the favorable scaling regime, $N < N_c \propto \log(1/\mathcal{E})$, grows with the inverse error threshold $\mathcal{E}$, in agreement with the results shown in Fig. 2(c-d). The advantage of importance sampling is thus most pronounced at high accuracy (small $\mathcal{E}$), enabling estimation of the purities with exponentially less measurements compared to uniform sapling.

We have demonstrated that importance sampling provides an exponential reduction of the measurement budget for two specific states, product and GHZ states, which are 'well-conditioned states' , and whose fidelity can be efficiently estimated via direct fidelity estimation [41, 42]. However, importance sampling is not useful only for these states. First, we show in the SM [31] a scaling analysis for pure random states that show a significant gain in using importance sampling compared to uniform sampling, which is here however constant with N. Second, we can also use our protocol to probe mixed, and highly entangled states, which are created via a quantum quench [25]. Here, we consider a state modelling a trapped-ion $10-$qubit experiment described in Ref. [25], which corresponds to the dynamics of a long-range XY Hamiltonian [43]. This highly entangled state is characterized by a purity of $p_2 \approx 0.62$, and a half-system purity of $p_2' \approx 0.16$, in agreement with the experimentally measured values [25]. In order to mimic a situation when the decoherence parameters are unknown, we train our neural network on an ideal pure state, i.e., modelling the system without errors, and use it to estimate the purity of the mixed state ρ. The results are shown in Fig. 3. While we see a clear improvement w.r.t uniform sampling, here importance sampling does not achieve the level of performance seen for GHZ states and product states. This is due to an imperfect training of the used convolutional neural network (CNN). While the training can obviously be improved by changing the structure of the neural network, we propose now a 'physics-motivated' complementary approach based on tensor networks, and which offers for this particular state an improvement over ML and provides a simplified approach to build $X_{\rm IS}$.

Importance sampling from Matrix-Product-States– We illustrate how we can use approximate theory representation for importance sampling. Here, we consider Matrix-Product-States (MPS), which have been introduced to solve numerically condensed-matter problems [35]. With N qubits, MPS are wavefunctions of the form

$$|\psi_D\rangle = \sum_{\substack{s_1,\ldots,s_N \\ \ell_1,\ldots,\ell_{N-1}}} [A_1]^{(\ell_1)}_{s_1} [A_2]^{(\ell_1,\ell_2)}_{s_2} \ldots [A_N]^{(\ell_{N-1})}_{s_N} |\mathbf{s}\rangle\,, \quad (4)$$

with $|\mathbf{s}\rangle = |s_1\rangle \otimes \ldots |s_N\rangle$, and where each 'bond' index ℓ_i can take at most D different values. A schematic of the sequence of $2, 3$ leg tensor A_i representing the MPS is shown in Fig. 1. The bond dimension D is the key parameter of a MPS, setting the maximum entanglement entropy $\propto \log(D)$ that can be captured by such state [35]. MPS are in particular relevant for approximating ground states of a many-body Hamiltonians [28, 35]. The MPS framework thus appears as a 'physically-inspired' approach to build an importance sampling function $X_{\rm IS}(u)$, which complements the ML approach (c.f., Fig. 1.). The training of $X_{\rm IS}(u)$ here is straightforward: (i.1) Form via a MPS algorithm an approximation $|\psi_D\rangle\langle\psi_D|$ of the quantum state ρ [35]. (i.2) Build the function $X_{\rm IS}(u)$ with Eq. (1), by realizing projective measurements $(s_u^k)_D$ on the MPS. While this step can be realized efficiently [44], here we simply use the probabilities $[P_u(s)]_D$ to build $X_{\rm IS}(u)$.

As shown in Fig. 3a), importance sampling with a MPS with $D = 15$ already provides a reduction of statistical errors compared to our best neural network model, while the fidelity $\langle\psi_D|\,\rho\,|\psi_D\rangle = 0.7$ shows that this MPS is indeed only an approximation of ρ. Here, $|\psi_D\rangle$ was formed by an algorithm that approximates the dynamics of a system with long-range interactions [45], see also Ref. [25]. When using MPS importance sampling, an interesting trade-off appears in terms of required classical versus quantum hardware to measure entanglement:

MPS with increasing bond dimensions require more classical resources, but are more performant for importance sampling. This is shown in Fig. 3b), where the statistical error is represented as a function of D. As shown in the SM [31], we can draw the same conclusions when considering subsystems of 5 and 10 qubits being part of a 10 and 20 qubit system, respectively.

Conclusion— Importance sampling boosts the power of randomized measurements protocols, allowing for measuring more efficiently purities and second Rényi entropies. Our approach is immediately applicable in all randomized measurement protocols, e.g. to measure scrambling [18], topological invariants [21, 22] , and fidelities [23, 41, 42].

We have studied how the investment of classical resources for building an importance sampling function 'pays off' in terms of statistical errors. We believe that further studies extending our scaling analysis can help us to answer this conceptual question, but also to again push the limits of randomized measurements.

Finally, as an extension of our protocol, it would be interesting to consider an adaptive measurement scheme, where the distribution p_{IS} is iteratively adapted based on prior measurements.

We thank A. Minguzzi, C. Branciard, M. Dalmonte for fruitful discussions, and comments on the manuscript. AR is supported by Laboratoire d'excellence LANEF in Grenoble (ANR-10-LABX-51-01) and from the Grenoble Nanoscience Foundation. BV acknowledges funding from the Austrian Science Fundation (FWF, P 32597 N), and the French National Research Agency (ANR-20-CE47-0005, JCJC project QRand). Work at Innsbruck is supported by the European Union program Horizon 2020 under Grants Agreement No. 817482 (PASQuanS) and No. 731473 (QuantERA via QTFLAG), the US Air Force Office of Scientific Research (AFOSR) via IOE Grant No. FA9550-19-1-7044 LASCEM, by the Simons Collaboration on Ultra-Quantum Matter, which is a grant from the Simons Foundation (651440, PZ), and by the Institut für Quanteninformation. A.E. acknowledges funding by the German National Academy of Sciences Leopoldina under the grant number LPDS 2021-02. We used ML routines of TensorFlow-Keras, ITensor MPS algorithms [46], and the quantum toolbox QuTiP [47].

[1] F. Arute, K. Arya, R. Babbush, D. Bacon, J. C. Bardin, R. Barends, R. Biswas, S. Boixo, F. G. S. L. Brandao, D. A. Buell, *et al.*, Nature **574**, 505 (2019).
[2] S. Ebadi, T. T. Wang, H. Levine, A. Keesling, G. Semeghini, A. Omran, D. Bluvstein, R. Samajdar, H. Pichler, W. W. Ho, and et al., Nature **595**, 227232 (2021).
[3] P. Scholl, M. Schuler, H. J. Williams, A. A. Eberharter, D. Barredo, K.-N. Schymik, V. Lienhard, L.-P. Henry, T. C. Lang, T. Lahaye, and et al., Nature **595**, 233238 (2021).
[4] S. J. Van Enk and C. W. Beenakker, Phys. Rev. Lett. **108**, 110503 (2012).
[5] M. C. Tran, B. Dakić, W. Laskowski, and T. Paterek, Phys. Rev. A **94**, 042302 (2016).
[6] A. Elben, B. Vermersch, M. Dalmonte, J. I. Cirac, and P. Zoller, Phys. Rev. Lett. **120**, 050406 (2018).
[7] B. Vermersch, A. Elben, M. Dalmonte, J. I. Cirac, and P. Zoller, Phys. Rev. A **97**, 023604 (2018).
[8] A. Elben, B. Vermersch, C. F. Roos, and P. Zoller, Phys. Rev. A **99**, 052323 (2019).
[9] L. Knips, J. Dziewior, W. Kłobus, W. Laskowski, T. Paterek, P. J. Shadbolt, H. Weinfurter, and J. D. A. Meinecke, npj Quant. Inf. **6**, 51 (2020).
[10] A. Ketterer, N. Wyderka, and O. Gühne, Phys. Rev. Lett. **122**, 120505 (2019).
[11] H.-Y. Huang, R. Kueng, and J. Preskill, Nat. Phys. **16**, 1050 (2020).
[12] A. Elben, R. Kueng, H.-Y. R. Huang, R. van Bijnen, C. Kokail, M. Dalmonte, P. Calabrese, B. Kraus, J. Preskill, P. Zoller, and B. Vermersch, Phys. Rev. Lett. **125**, 200501 (2020).
[13] Y. Zhou, P. Zeng, and Z. Liu, Phys. Rev. Lett. **125**, 200502 (2020).
[14] A. Ketterer, N. Wyderka, and O. Gühne, Quantum **4**, 325 (2020).
[15] A. Ketterer, S. Imai, N. Wyderka, and O. Gühne, arXiv:2012.12176.
[16] V. Vitale, A. Elben, R. Kueng, A. Neven, J. Carrasco, B. Kraus, P. Zoller, P. Calabrese, B. Vermersch, and M. Dalmonte, arXiv:2101.07814.
[17] S. Imai, N. Wyderka, A. Ketterer, and O. Gühne, Phys. Rev. Lett. **126**, 150501 (2021).
[18] B. Vermersch, A. Elben, L. M. Sieberer, N. Y. Yao, and P. Zoller, Phys. Rev. X **9**, 021061 (2019).
[19] X.-L. Qi, E. J. Davis, A. Periwal, and M. Schleier-Smith, arXiv:1906.00524.
[20] R. J. Garcia, Y. Zhou, and A. Jaffe, Phys. Rev. Research **3**, 033155 (2021).
[21] A. Elben, J. Yu, G. Zhu, M. Hafezi, F. Pollmann, P. Zoller, and B. Vermersch, Sci. Adv. **6**, eaaz3666 (2020).
[22] Z.-P. Cian, H. Dehghani, A. Elben, B. Vermersch, G. Zhu, M. Barkeshli, P. Zoller, and M. Hafezi, Phys. Rev. Lett. **126**, 050501 (2021).
[23] A. Elben, B. Vermersch, R. van Bijnen, C. Kokail, T. Brydges, C. Maier, M. K. Joshi, R. Blatt, C. F. Roos, and P. Zoller, Phys. Rev. Lett. **124**, 010504 (2020).
[24] D. Gross, Y. K. Liu, S. T. Flammia, S. Becker, and J. Eisert, Phys. Rev. Lett. **105**, 150401 (2010).
[25] T. Brydges, A. Elben, P. Jurcevic, B. Vermersch, C. Maier, B. P. Lanyon, P. Zoller, R. Blatt, and C. F. Roos, Science **364**, 260 (2019).
[26] M. K. Joshi, A. Elben, B. Vermersch, T. Brydges, C. Maier, P. Zoller, R. Blatt, and C. F. Roos, Phys. Rev. Lett. **124**, 240505 (2020).
[27] R. Horodecki and M. Horodecki, Phys. Rev. A **54**, 1838 (1996).
[28] J. Eisert, M. Cramer, and M. B. Plenio, Rev. Mod. Phys. **82**, 277 (2010).
[29] K. J. Satzinger, Y. Liu, A. Smith, C. Knapp, M. Newman, C. Jones, Z. Chen, C. Quintana, X. Mi, A. Dunsworth, C. Gidney, I. Aleiner, F. Arute, K. Arya, J. Atalaya, R. Babbush, J. C. Bardin, R. Barends,

J. Basso, A. Bengtsson, A. Bilmes, M. Broughton, B. B. Buckley, D. A. Buell, B. Burkett, N. Bushnell, B. Chiaro, R. Collins, W. Courtney, S. Demura, A. R. Derk, D. Eppens, C. Erickson, E. Farhi, L. Foaro, A. G. Fowler, B. Foxen, M. Giustina, A. Greene, J. A. Gross, M. P. Harrigan, S. D. Harrington, J. Hilton, S. Hong, T. Huang, W. J. Huggins, L. B. Ioffe, S. V. Isakov, E. Jeffrey, Z. Jiang, D. Kafri, K. Kechedzhi, T. Khattar, S. Kim, P. V. Klimov, A. N. Korotkov, F. Kostritsa, D. Landhuis, P. Laptev, A. Locharla, E. Lucero, O. Martin, J. R. McClean, M. McEwen, K. C. Miao, M. Mohseni, S. Montazeri, W. Mruczkiewicz, J. Mutus, O. Naaman, M. Neeley, C. Neill, M. Y. Niu, T. E. O'Brien, A. Opremcak, B. Pat, A. Petukhov, N. C. Rubin, D. Sank, V. Shvarts, D. Strain, M. Szalay, B. Villalonga, T. C. White, Z. Yao, P. Yeh, J. Yoo, A. Zalcman, H. Neven, S. Boixo, A. Megrant, Y. Chen, J. Kelly, V. Smelyanskiy, A. Kitaev, M. Knap, F. Pollmann, and P. Roushan, "Realizing topologically ordered states on a quantum processor," (2021), arXiv:2104.01180 [quant-ph].

[30] D. Zhu, Z.-P. Cian, C. Noel, A. Risinger, D. Biswas, L. Egan, Y. Zhu, A. M. Green, C. H. Alderete, N. H. Nguyen, Q. Wang, A. Maksymov, Y. Nam, M. Cetina, N. M. Linke, M. Hafezi, and C. Monroe, "Cross-platform comparison of arbitrary quantum computations," (2021), arXiv:2107.11387 [quant-ph].

[31] See Supplemental Material, which includes Refs. 6, 8, 13, 25.

[32] P. Diaconis and P. J. Forrester, arXiv:1512.09229.

[33] M. Planitz, W. H. Press, B. P. Flannery, S. A. Teukolsky, and W. T. Vetterling, *Numerical Recipes: The Art of Scientific Computing*, 3rd ed., Vol. 71 (Cambridge University Press, New York, NY, USA, 1987).

[34] In the examples below, we have $X_{\rm IS} \approx X(u) > 0$.

[35] U. Schollwöck, Annals of Physics **326**, 96 (2011).

[36] M. Cramer, M. B. Plenio, S. T. Flammia, R. Somma, D. Gross, S. D. Bartlett, O. Landon-Cardinal, D. Poulin, and Y.-K. Liu, Nat. Comm. **1**, 149 (2010).

[37] G. Torlai, G. Mazzola, J. Carrasquilla, M. Troyer, R. Melko, and G. Carleo, Nat. Phys. **14**, 447 (2018).

[38] G. Torlai, B. Timar, E. P. L. van Nieuwenburg, H. Levine, A. Omran, A. Keesling, H. Bernien, M. Greiner, V. Vuletić, M. D. Lukin, R. G. Melko, and M. Endres, Phys. Rev. Lett. **123**, 230504 (2019).

[39] C. Kokail, R. van Bijnen, A. Elben, B. Vermersch, and P. Zoller, Nature Physics **17**, 936942 (2021).

[40] G. Carleo and M. Troyer, Science **355**, 602 (2017).

[41] S. T. Flammia and Y.-K. Liu, Phys. Rev. Lett. **106**, 230501 (2011).

[42] M. P. da Silva, O. Landon-Cardinal, and D. Poulin, Phys. Rev. Lett. **107**, 210404 (2011).

[43] The precise master equation is given in Ref. [25], the propagation time is $t = 5$ ms.

[44] Z.-Y. Han, J. Wang, H. Fan, L. Wang, and P. Zhang, Phys. Rev. X **8**, 31012 (2018).

[45] M. P. Zaletel, R. S. Mong, C. Karrasch, J. E. Moore, and F. Pollmann, Phys. Rev. B **91**, 165112 (2015), 1407.1832.

[46] M. Fishman, S. R. White, and E. M. Stoudenmire, arXiv:2007.14822.

[47] J. Johansson, P. Nation, and F. Nori, Comput. Phys. Commun. **184**, 1234 (2013).